Journal of Hepatocellular Carcinoma

Dovepress
Taylor & Francis Group

Open Access Full Text Article

ORIGINAL RESEARCH

MRI Features and Neutrophil-to-Lymphocyte Ratio (NLR)-Based Nomogram to Predict Prognosis of Microvascular Invasion-Negative Hepatocellular Carcinoma

Yunyun Wei[1,2,*], Xuegang Huang[3,*], Wei Pei[1,2,*], Yang Zhao[1,2], Hai Liao[1,2]

[1]Department of Medical Imaging Center, Guangxi Medical University Cancer Hospital, Nanning, Guangxi, 530021, People's Republic of China; [2]Guangxi Key Clinical Specialty (Medical Imaging Department), Nanning, Guangxi, 530021, People's Republic of China; [3]Department of Infectious Diseases, The First People's Hospital of Fangchenggang City, Fangchenggang, Guangxi, 538021, People's Republic of China

*These authors contributed equally to this work

Correspondence: Hai Liao, Department of Medical Imaging Center, Guangxi Medical University Cancer Hospital, No. 71 hedi Road, Nanning, Guangxi, 530021, People's Republic of China, Tel +86-771-5334951, Email 42442427@qq.com

Purpose: This study aimed to develop a novel nomogram to predict recurrence-free survival (RFS) for microvascular invasion (MVI)-negative hepatocellular carcinoma (HCC) patients after curative resection.

Patients and Methods: A total of 143 pathologically confirmed MVI-negative HCC patients were analyzed retrospectively. Baseline MRI features and inflammatory markers were collected. We used univariable and multivariable Cox regression analysis to identify the independent risk factors for RFS. And we established a nomogram based on significant MRI features and inflammatory marker. The receiver operating characteristic (ROC) curve, concordance index (C-index) and calibration curve were used to evaluate the predictive accuracy and discriminative ability of the nomogram. The decision curve analysis (DCA) was performed to validate the clinical utility of the nomogram.

Results: In multivariate Cox regression analysis, neutrophil-to-lymphocyte ratio (NLR) (P = 0.018), tumor size (P = 0.002), and tumor capsule (P = 0.000) were independent significant variables associated with RFS. Nomogram with independent factors was developed and achieved a good C-index of 0.730 (95% confidence interval [CI]: 0.656–0.804) for predicting RFS. In ROC analysis, the areas under curve of the nomogram for 1-, 3- and 5-year RFS prediction were 0.725, 0.784 and 0.798, respectively. The risk score calculated by nomogram could divide MVI-negative HCC patients into high-risk group or low-risk group (P < 0.0001). DCA analysis revealed that the nomogram could increase net benefit and exhibited a wider range of threshold probabilities by the risk stratification than the independent risk factors in the prediction of MVI-negative HCC recurrence.

Conclusion: The nomogram prognostic model based on MRI features and NLR for predicting RFS showed high accuracy in MVI-negative HCC patients after curative resection. It can help clinicians make treatment decisions for MVI-negative HCC patients and identify high-risk patients for timely intervention.

Plain Language Summary: The lack of prognostic studies for microvascular invasion (MVI)-negative HCC patients after hepatectomy poses a great challenge to clinical management. To bridge this gap, our team conducted extensive research and developed a customized prognostic nomogram specifically for this patient subgroup. We created a predictive model that relies on MRI features (tumor size and tumor capsule) and neutrophil-to-lymphocyte ratio (NLR). This model demonstrates high accuracy in predicting outcomes for MVI-negative HCC patients following curative resection. And our model aids clinicians in making treatment decisions for MVI-negative HCC patients and in identifying high-risk patients for timely intervention.

Keywords: hepatocellular carcinoma, microvascular invasion-negative, neutrophil-to-lymphocyte ratio, recurrence-free survival

Received: 14 July 2024
Accepted: 8 February 2025
Published: 15 February 2025

Introduction

Liver cancer is the sixth most common malignancy and the third leading cause of cancer-related death worldwide, according to 2022 global cancer statistics.[1] Hepatocellular carcinoma (HCC) accounts for 75–85% of liver cancer. For HCC patients, hepatic resection has been the mainstay of curative treatment. But the 5-year recurrence rate after surgery is as high as 70%, which is the main cause of poor prognosis for HCC patients.[2]

Microvascular invasion (MVI) is a robust predictor for HCC recurrence after hepatectomy.[3] It plays a crucial role in therapeutic decision-making, such as opting for surgery instead of ablation,[4] selecting a wider surgical margin at hepatectomy, more intensive postoperative monitoring,[5] and considering adjuvant therapies.[6] However, MVI has been reported in only about 15–57% of HCC,[4–7] and many MVI-negative patients still experience postoperative recurrence in clinical practice. This suggests that research on the prognosis of MVI-negative HCC patients should be carried out to help the clinic fully understand and deal with the potential recurrence risk.

MRI has been widely used for the diagnosis and assessment of HCC. Prior works explored some imaging features, such as tumor size, tumor capsule, mosaic architecture, and Liver Imaging Reporting and Data System (LI-RADS), which can serve as noninvasive risk factors to evaluate the aggressive biological behavior of HCC.[7–9] Additionally, systemic inflammation is a key risk factor for HCC progression and poor outcomes. Inflammation can enhance tumor progression and immune evasion.[10,11] Therefore, an HCC-promoting state can be suspected from high levels of inflammatory markers, thus resulting in a poor prognosis. Inflammatory markers like the neutrophil-to-lymphocyte ratio (NLR), platelet-to-lymphocyte ratio (PLR), lymphocyte-to-monocyte ratio (LMR), and systemic immune inflammation index (SII), have been correlated with worse survival outcomes in HCC patients.[12–14] But to the best of our knowledge, only a few studies have explored the relationship between MRI imaging features and prognosis in MVI-negative HCC patients.[15–18] Moreover, these studies have been limited by their short follow-up periods and a lack of emphasis on inflammatory markers. It's also important to note that the nomogram, a tool that combines various prognostic and decisive factors to calculate individual numerical probabilities for clinical outcomes, satisfies the clinical need for comprehensive biological and clinical models.[19] It also aligns with the goal of personalized medicine and has been extensively used in the prognostic evaluation of HCC patients.[15–18]

Therefore, we hypothesized that the certain MRI features and inflammatory markers were associated with recurrence-free survival (RFS) of MVI-negative HCC patients. We believed that when these factors were incorporated into a nomogram model, it could accurately predict prognosis and offer significant clinical application.

Materials and Methods

Patients

This retrospective study performed at a single medical institution. Ethics committee approval was granted by our institutional review board, which waived the requirement for informed consent. And this study was conducted in accordance with the Declaration of Helsinki.

Between January 2014 and November 2018, a total of 143 MVI-negative HCC patients who underwent dynamic contrast-enhanced MRI followed by curative hepatectomy were included. The inclusion criteria were as follows: (1) patients with MVI-negative HCC confirmed by histopathologic examination; (2) patients treated by resection with tumor-negative resection margins (R0 resection); (3) MRI quality was adequate for analysis. The exclusion criteria were as follows: (1) patients have two or more HCC lesions; (2) HCC tumor size larger than 10 cm; (3) patients treated by prior cancer-related treatment before surgery; (4) patients with other malignant tumors; (5) those that were lost to death, and lost to follow-up within 5 years. Figure 1 displays the flowchart detailing the selection of eligible patients.

MRI Acquisition and Imaging Analysis

MRI was performed on a 1.5-T system (Magnetom Avanto, Siemens Healthcare, Erlangen, Germany). Baseline MRI included a T1-weighted sequence, a T2-weighted and T2-weighted fat-suppressed sequence. For gadolinium- diethylenetriamine pentaacetic acid (Gd-DTPA, 0.1 mmol/kg of body weight; Magnevist, Schering, Berlin, Germany)-enhanced MRI, arterial phase (25−30 seconds), portal venous phase (55−65 seconds), and delayed phase (2 mins) were obtained by

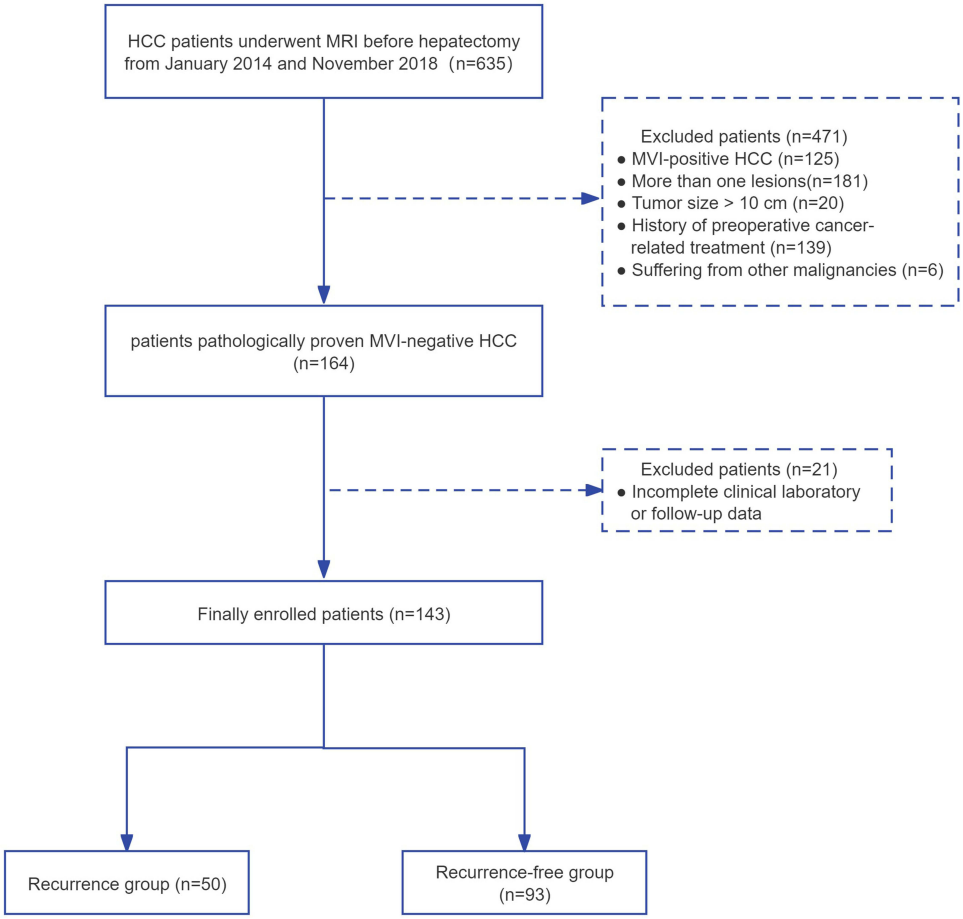

Figure 1 Flowchart of this study population.
Abbreviations: HCC, hepatocellular carcinoma; MVI, microvascular invasion.

using a T1-weighted three-dimensional turbo-field-echo sequence. The acquisition parameters are listed in Supplementary Table S1.

Images were independently analyzed by two radiologists (H.L. and Y.W, with 16 and 6 years of experience in abdominal imaging, respectively) who were blinded to clinical, histological, and laboratory, and follow-up results. For discordant cases, the two reviewers met to discuss and draw final conclusions by consensus.

The two reviewers independently evaluated some imaging features for each HCC as defined in LI-RADS v2018,[20] including major imaging features (including tumor size, non-rim arterial phase hyperenhancement [APHE], non-peripheral washout, and enhancing capsule), ancillary imaging features (including mosaic architecture, nodule-in-nodule architecture, fat in mass, and blood products in mass), two non-LI-RADS imaging features (non-smooth tumor margin and tumor capsule).

Nonsmooth tumor margin was defined as non-nodular tumors with extranodular extension that had a budding portion at its periphery protruding into the liver parenchyma or multinodular confluence appearance.[8] Complete tumor capsule was defined as complete peripheral rim of smooth hyperenhancement in the portal venous or delayed phase. Incomplete or without tumor capsule was defined as the absence of "capsule" or the presence of a disrupted "capsule" in any imaging plane.[21] Enhancing capsule was defined as a linear enhancing rim surrounding the tumor in the portal venous or delayed phase, including both complete and incomplete rims.[22]

https://doi.org/10.2147/JHC.S486955

Clinical Data Acquisition

The following clinical data were analyzed: age; gender; drink; HBsAg, body mass index (BMI); liver cirrhosis and Edmondson-Steiner grade. In addition, the laboratory results were collected, including: alpha-fetoprotein (AFP; < 400 or ≥ 400 ng/mL); neutrophil-to-lymphocyte ratio (NLR; < 2 or ≥ 2); platelet-to-lymphocyte ratio (PLR; < 150 or ≥ 150); lymphocyte-to-monocyte ratio (LMR; < 4 or ≥ 4); systemic immune inflammation index (SII); white blood cell (WBC); platelet (PLT; < 100 or ≥ 100); neutrophils (Neu); alanine aminotransferase (ALT; ≤ 40 or > 40 U/L); and aspartate aminotransferase (AST; ≤ 40 or > 40 U/L).

Follow-Up

Postoperatively, all patients received standardized clinical and radiologic follow-up according to the institutional protocol. The surveillance program consisted of laboratory tests including AFP, liver function and ultrasound examination, performed every 1 month for the first year after surgery and then every 3 months. Additionally, contrast-enhanced CT or MRI was performed every 3–6 months. The primary end point was tumor recurrence. RFS was calculated from the date of curative resection to the date of recurrence or death or the most recent follow-up. The mean follow-up period was 55 months (range, 2–96 months).

Statistical Analysis

The Chi-square or Fisher's exact test were used to compare categorical variables. The Mann–Whitney *U*-test was used for continuous variables. Independent prognostic factors of RFS were identified by univariate and multivariate Cox proportional hazards regression analysis. Subsequently, a nomogram was constructed on the results of multivariable Cox regression analysis. The receiver operating characteristic (ROC) curve, concordance index (C-index) and calibration curve were used to evaluate the predictive accuracy and discriminative ability of the nomogram. Each patient was assigned a total risk score (NomoScore: nomogram risk score) for risk stratification of RFS according to the nomogram model. Patients were divided into different risk groups (low- or high-risk group) to identify significant differences in RFS between the groups. Decision curve analysis (DCA) was conducted to determine the clinical benefit of the nomogram by quantifying the net benefit along with the increase in threshold probabilities.

All statistical analyses were performed by using statistical SPSS (version 22.6; IBM Corp., Armonk, NY, USA); and R version 3.6.3 (http://www.r-project.org/). Differences with a P-value < 0.05 were considered statistically significant.

Results

Clinical Characteristics and Recurrence

Baseline and clinicopathological features of 143 patients with solitary MVI-Negative HCC Patients (113 males and 30 females; mean age: 51.4 ± 11.3 years; range: 24–76 years) are summarized in Table 1.

At the end of the follow-up period, 50 patients experienced recurrence and 93 patients were free of recurrence. The median follow-up time was 55 months (2–96 months). The cumulative 1-, 3-, and 5-year RFS rates were 86%, 75%, and 68%, respectively.

After comparing the baseline data of recurrence group (n = 50) and recurrence-free group (n = 93), correlation analysis showed that there were significant differences in drink (P = 0.028), NLR ≥ 2 (P = 0.014), tumor size (P = 0.010), tumor capsule (P = 0.001), and mosaic architecture (P = 0.004) between the groups (Table 1).

Development and Validation of Nomogram Prediction Model

In univariable Cox analysis, postoperative recurrence was associated with five predictors: NLR ≥ 2 (P = 0.014), drink (P = 0.049), tumor size (P = 0.001), tumor capsule (P = 0.000), and mosaic architecture (P = 0.001) (Table 2). In multivariable analysis, NLR ≥ 2 (hazard ratio [HR]: 1.999; P = 0.018), tumor size (HR: 1.236; P = 0.002), and tumor capsule (HR: 3.409; P = 0.000) were independent significant variables associated with tumor recurrence (Table 2) (Figures 2 and 3).

Table 1 Baseline and Clinicopathological Characteristics of MVI-Negative HCC Patients

Variables	Total (n=143)	Recurrence Group (n=50)	Recurrence-Free Group (n=93)	*P*-value
Age	51.4±11.3	50.5±11.0	52.0±11.5	0.528
Gender				0.833
Female	30 (21.0)	10 (20.0)	20 (21.5)	
Male	113 (79.0)	40 (80.0)	73 (78.5)	
Drink				0.028*
No	102 (71.3)	30 (60.0)	72 (77.4)	
Yes	41 (28.7)	20 (40.0)	21 (22.6)	
HBsAg				0.670
Negative	15 (10.5)	4 (8.0)	11 (11.8)	
Positive	128 (89.5)	46 (92.0)	82 (88.2)	
BMI	23.2±3.7	23.7±3.7	22.9±3.6	0.193
Liver cirrhosis				0.099
No	59 (41.3)	16 (32.0)	43 (46.2)	
Yes	84 (58.7)	34 (68.0)	50 (53.8)	
Edmondson-Steiner grade				0.473
Well differentiated	7 (4.9)	1 (2.0)	6 (6.5)	
Moderately differentiated	83 (58.0)	29 (58.0)	54 (58.1)	
Poorly differentiated	53 (37.1)	20 (40.0)	33 (35.5)	
AFP (ng/mL)				0.306
<400	110 (76.9)	36 (72.0)	74 (79.6)	
≥ 400	33 (23.1)	14 (28.0)	19 (20.4)	
NLR				0.014*
<2	80 (55.9)	21 (42.0)	59 (63.4)	
≥ 2	63 (44.1)	29 (58.0)	34 (36.6)	
PLR				0.203
<150	118 (82.5)	38 (76.0)	80 (86.0)	
≥ 150	25 (17.5)	12 (24.0)	13 (14.0)	
LMR				0.164
<4	52 (36.4)	22 (44.0)	30 (32.3)	
≥ 4	91 (63.6)	28 (56.0)	63 (67.7)	
SII	528.8±1216.2	824.3±285.7	369.9±23.8	0.182
WBC ($\times 10^9$/L)	6.1±2.1	6.6±0.4	5.9±0.2	0.552
PLT ($\times 10^9$/L)				0.063

(*Continued*)

https://doi.org/10.2147/JHC.S486955

Table 1 (Continued).

Variables	Total (n=143)	Recurrence Group (n=50)	Recurrence-Free Group (n=93)	*P*-value
<100	15 (10.5)	2 (4.0)	13 (14.0)	
≥ 100	128 (89.5)	48 (96.0)	80 (86.0)	
Neu ($\times 10^9$/L)	4.7±13.5	7.3±3.2	3.3±0.1	0.069
ALT (U/L)				0.995
≤ 40	93 (65.0)	32 (64.0)	61 (65.6)	
>40	50 (35.0)	18 (36.0)	32 (34.4)	
AST (U/L)				1.000
≤ 40	93 (65.0)	33 (66.0)	62 (66.7)	
>40	50 (35.0)	17 (34.0)	31 (33.3)	
MRI findings				
Tumor size (cm)	4.28±2.02	4.91±2.19	3.94±1.86	0.010*
Nonsmooth tumor margin				0.067
Absent	75 (52.4)	21 (42.0)	54 (58.1)	
Present	68 (47.6)	29 (58.0)	39 (41.9)	
Tumor capsule				0.001*
Complete	73 (51.0)	16 (32.0)	57 (61.3)	
Incomplete/Without	70 (49.0)	34 (68.0)	36 (38.7)	
APHE				0.449
Absent	12 (8.4)	3 (6.0)	9 (9.7)	
Present	131 (91.6)	47 (94.0)	84 (90.3)	
Washout				0.945
Absent	31 (21.7)	11 (22.0)	20 (21.5)	
Present	112 (78.3)	39 (78.0)	73 (78.5)	
Enhancing capsule				0.070
Absent	21 (14.7)	11 (22.0)	10 (10.8)	
Present	122 (85.3)	39 (78.0)	83 (89.2)	
Mosaic architecture				0.004*
Absent	92 (64.3)	24 (48.0)	68 (73.1)	
Present	51 (35.7)	26 (52.0)	25 (26.9)	
Nodule-in-nodule architecture				1.000
Absent	24 (16.8)	8 (16.0)	16 (17.2)	
Present	119 (83.2)	42 (84.0)	77 (82.8)	

(*Continued*)

Table 1 (Continued).

Variables	Total (n=143)	Recurrence Group (n=50)	Recurrence-Free Group (n=93)	*P*-value
Fat in mass				0.090
Absent	99 (69.2)	30 (60.0)	69 (74.2)	
Present	44 (30.8)	20 (40.0)	24 (25.8)	
Blood products				0.115
Absent	104 (72.7)	32 (64.0)	72 (77.4)	
Present	39 (27.3)	18 (36.0)	21 (22.6)	

Note: *Statistically significant variables with a P-value < 0.05.
Abbreviations: BMI, body mass index; AFP, alpha-fetoprotein; NLR, neutrophil-to-lymphocyte ratio; PLR, platelet-to-lymphocyte ratio; LMR, lymphocyte-to-monocyte ratio; SII, systemic immune inflammation index; WBC, white blood cell; PLT, platelet; Neu, neutrophils; ALT, alanine transaminase; AST, aspartate aminotransferase; APHE, arterial phase hyperenhancement.

Table 2 Univariate and Multivariate Cox Analyses for RFS of MVI-Negative HCC Patients

Variable	Univariate Analysis			Multivariate Analysis		
	HR	95% CI	*P*-value	HR	95% CI	*P*-value
NLR ≥ 2	2.029	1.156–3.561	0.014	1.999	1.126–3.546	0.018
Drink	0.566	0.321–0.997	0.049			
Tumor size (cm)	1.248	1.093–1.424	0.001	1.236	1.080–1.416	0.002
Tumor capsule	3.094	1.698–5.636	0.000	3.409	1.854–6.268	0.000
Mosaic architecture	2.594	1.482–4.539	0.001			

Abbreviation: NLR, neutrophil-to-lymphocyte ratio.

A Cox regression model-based nomogram was developed from these significant independent variables (Figure 4). The nomogram achieved a good C-index of 0.730 (95% CI: 0.656–0.804) by using bootstrapping to measure the discrimination in predicting 1-, 3-, and 5-year RFS rates. To evaluate the performance of the nomogram, the ROC curves were generated and the areas under curve (AUCs) were calculated. In ROC analysis, the AUCs of the nomogram for 1-, 3- and 5-year RFS prediction were 0.725, 0.784 and 0.798, respectively (Figure 5A). The calibration curves for 1-, 3- and 5-year RFS rates were

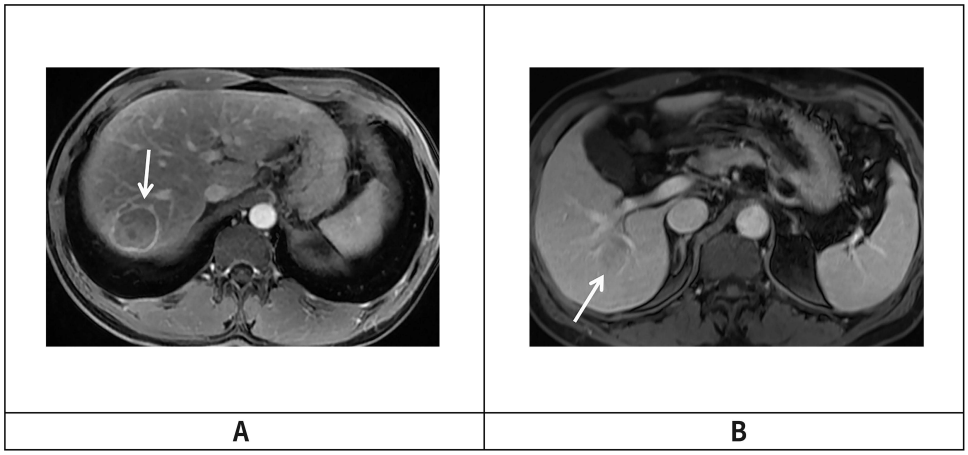

Figure 2 MRI images of MVI-negative HCC patients who did not relapse during follow-up. (**A**) Delayed phase image of a 44-year-old male patient showing a 3.5 cm mass (arrow) with complete capsule. Tumor recurrence has not been found after 70 months of follow-up. (**B**) Delayed phase image of a 60-year-old male patient showing a 2.6 cm mass (arrow) without capsule. Tumor recurrence has not been found after 71 months of follow-up.

https://doi.org/10.2147/JHC.S486955

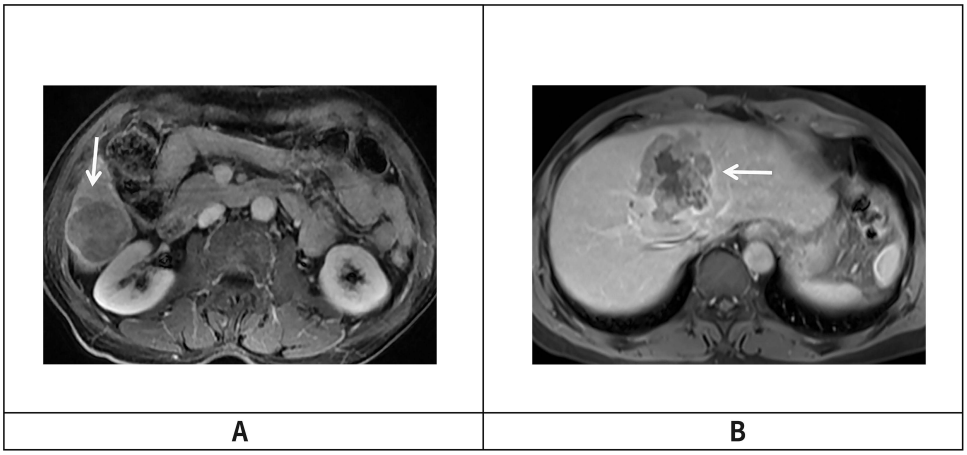

Figure 3 MRI images of MVI-negative HCC patients who relapsed within 5 years after surgery. (**A**) Delayed phase image of a 68-year-old male patient showing a 4.7 cm mass (arrow) with incomplete capsule. Tumor recurrence was detected 15 months after curative resection. (**B**) Delayed phase image of a 58-year-old male patient showing a 4.7 cm mass (arrow) with incomplete capsule. Tumor recurrence was detected 45 months after curative resection.

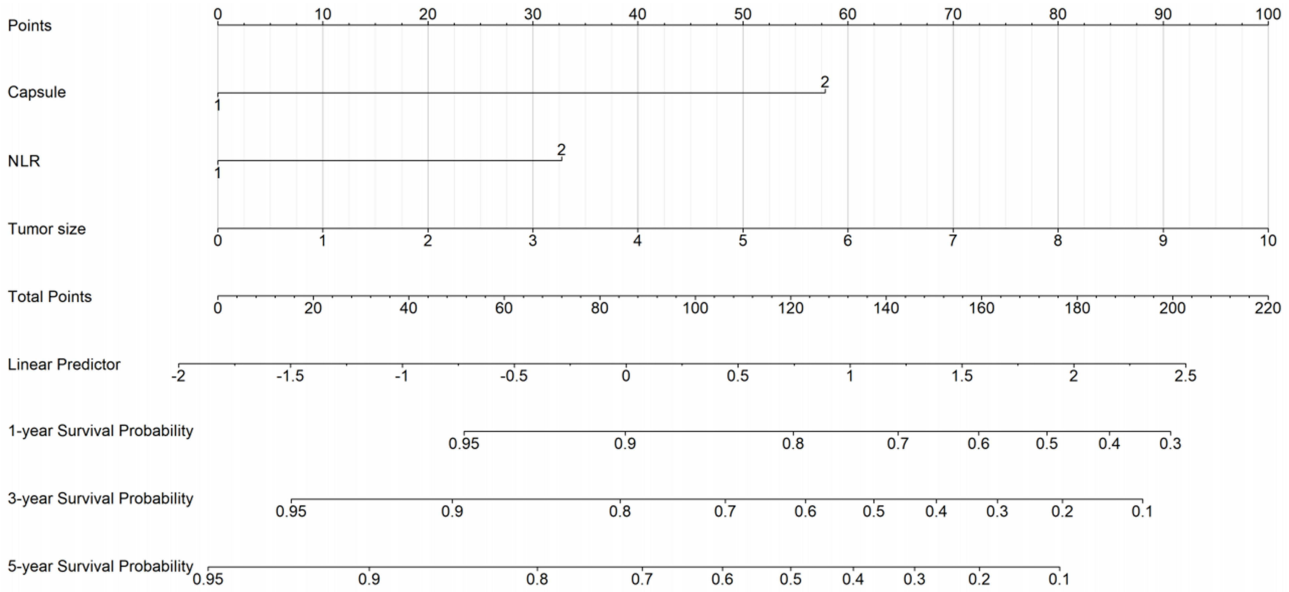

Figure 4 Nomogram for predicting 1-, 3-, and 5-year recurrence-free survival (RFS) in MVI-negative HCC patients after hepatectomy. Each independent prognostic factor identified in the Cox regression was assigned a point (complete capsule is assigned 0 point and incomplete/without capsule is assigned 58 points, neutrophil-to-lymphocyte ratio [NLR] < 2 is assigned 0 point and NLR ≥ 2 is assigned 33 points, tumor size is assigned 10 points per 1 cm). The total points could be obtained by calculating the sum of all factors. With the total points, the probabilities of 1-, 3- and 5-year RFS could be predicted.

largely overlapped with the standard lines (Figure 5B–D). The final nomogram could accurately distinguish the RFS of MVI-negative HCC patients and had better consistency between the predicted probability and the observed probability of RFS.

Prognostic Assessment and Risk Stratification

MVI-negative HCC patients were divided into high-risk group (NomoScore ≥ 109) or the low-risk group (NomoScore < 109) based on the total risk scores calculated by the nomogram model. Survival curves were calculated to compare the RFS rates between the two groups using the Kaplan–Meier method, and the results showed a significant discriminatory ability. ($P < 0.0001$, Figure 6A). DCA analysis showed that the nomogram could increase net benefit and exhibited a wider range of threshold probabilities than the independent risk factors (NLR, tumor size and tumor capsule) by the risk stratification (Figure 6B–D).

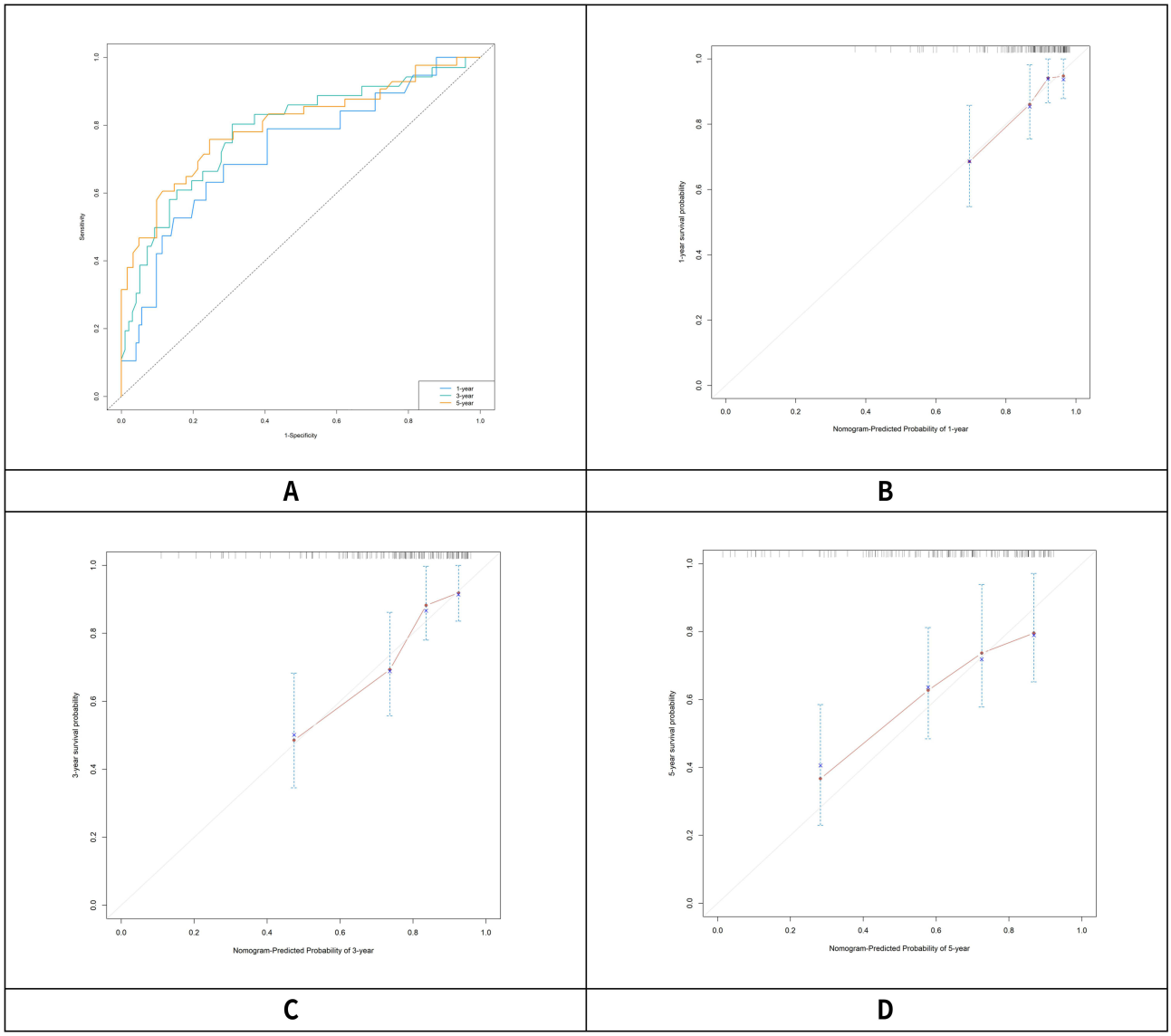

Figure 5 Evaluation of the performance of the nomogram. (**A**) Receiver operating characteristic curve for the nomogram model. (**B**–**D**) Calibration curves of nomogram for predicting 1-, 3-, and 5-year probability of recurrence-free survival (RFS).

Discussion

The lack of prognostic studies for MVI-negative HCC patients after hepatectomy poses a great challenge to clinical management. Therefore, our study specifically focused on MVI-negative patients, a subgroup that has rarely been investigated separately before, and aimed at constructing a prognostic nomogram designed for them.

Our study demonstrated that tumor size, tumor capsule and NLR were independent significant variables associated with RFS of MVI-negative HCC. And we developed an easy-to-use and effective nomogram model, which showed good predictive performance. Furthermore, the nomogram model was capable of stratifying patients into 2 prognostically distinct risk groups. This was clinically relevant because it may help to identify the patients at high risk of recurrence, for whom closer surveillance could be considered, and adjuvant therapies might provide survival benefit.

Previous studies have also confirmed that tumor size plays an important role in the prognosis of MVI-negative HCC patients.[15,17] Although there is no uniformity in the criteria for predicting recurrence based on tumor size, it is generally accepted that, as the tumor size increases, the risk of intrahepatic metastasis increases.[5]

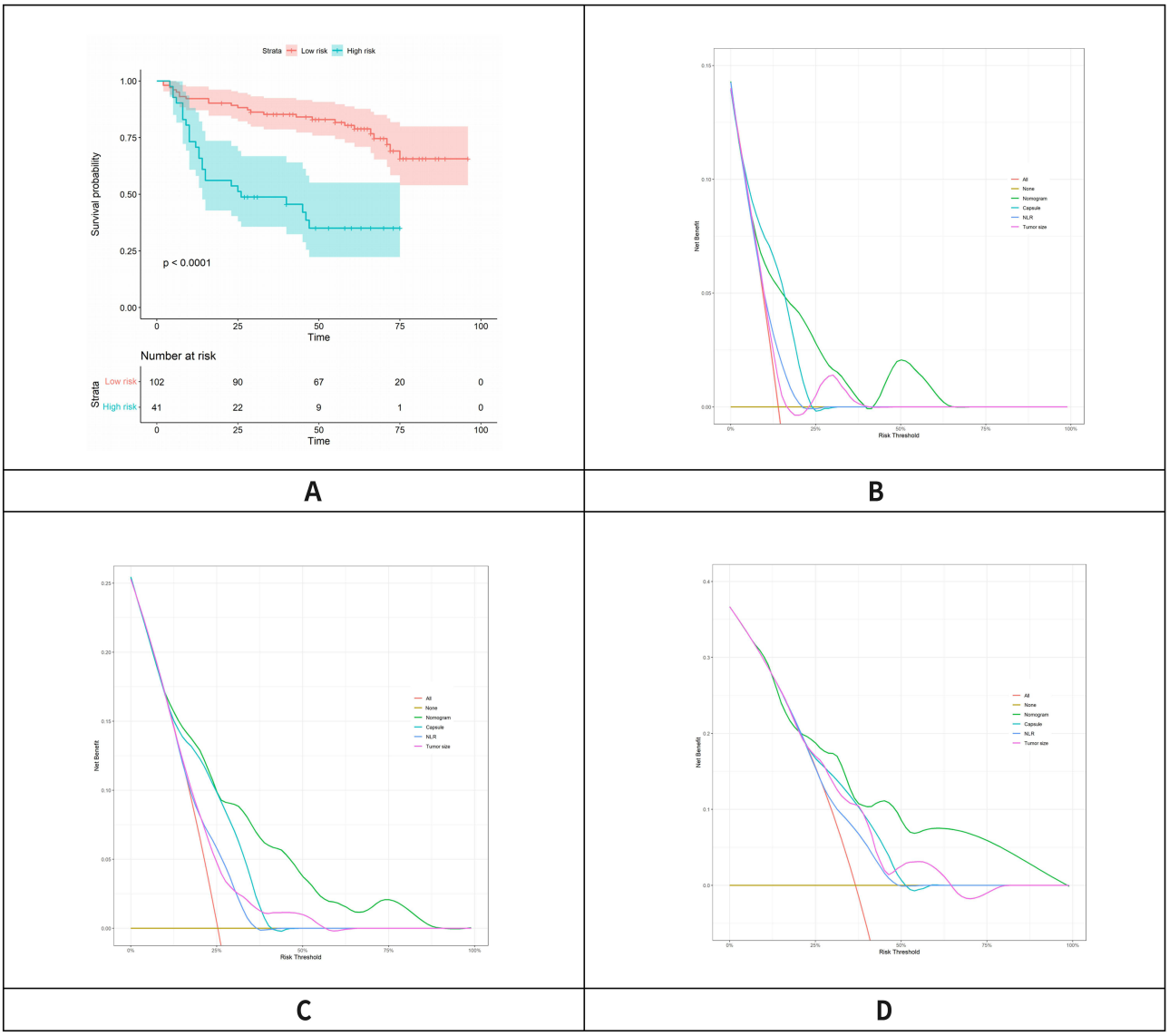

Figure 6 Prognostic assessment and risk stratification of the nomogram prediction model. (**A**) Risk stratification for recurrence-free survival (RFS). (**B**–**D**) Decision curve analyses of 1-, 3-, and 5-year RFS rates show an increase in net benefit.

The tumor capsule, as an imaging feature, refers to the hyperplastic fibrous connective tissues surrounding the tumor. It is actually a "pseudo-capsule" because it lacks epithelial tissues. But it may help to limit the growth of tumor.[23] Our study found that incomplete or without tumor capsule is an independent predictor of RFS, which is consistent with reports by Wei et al and Ng et al[21,23,24] A possible reason for this may be that, incomplete or without tumor capsule is associated with high BRAF and RAF1 expression in HCC, which can promote tumor invasion and metastasis.[25]

Interestingly, previous studies found that tumor size and tumor capsule are also indicators for MVI,[26–28] a significant risk factor of recurrence in HCC patients. Therefore, these imaging features can be used to predict MVI expression in HCC and thus to evaluate the prognosis of patients. However, in our study, we found a direct association between these two imaging features and postoperative recurrence in MVI-negative HCC patients. Hence, we propose that imaging features may reflect the gene expression patterns of the tumor, not just MVI. This perspective is consistent with earlier findings[3,29,30] and introduces a novel and innovative viewpoint that we have derived from similar researches.[16–18]

Findings from this study also contribute to elucidate the clinical value of inflammatory marker. Elevated NLR plays a crucial part in the progression of various malignancies.[12,31,32] Neutrophils are thought to drive tumor progression by enhancing tumor

cell survival, invasiveness and metastatic ability, immunosuppression, extracellular matrix remodeling, and angiogenesis.[33] While lymphocytes control tumor growth by secreting cytokines and inducing cytotoxic cell death, and the reduction of lymphocyte levels will damage the immune function of the host.[34] Moreover, high NLR might be linked with greater disease burden and liver dysfunction. Our study showed that NLR ≥ 2 is an independent prognosticator of poor RFS in MVI-negative HCC patients. This indicates that a higher NLR is associated with poorer survival outcomes, a finding that aligns with previous research.[12,14]

In this study, the dataset was not splitted into two groups randomly, a training group and a validation group. On the contrary, we only developed the internal validation of the nomogram with a representative sample size to avoid data waste and statistical inefficiency.

There are limitations in this study. First, this is a single-center study, and the selection bias is inevitable owing to the retrospective design. Second, as we only enrolled patients with a solitary HCC ≤ 10 cm, the results cannot be generalized to multiple tumors or tumors larger than 10 cm. Third, there are still some disputes about the optimal cut-off value of NLR, PLR and LMR, but our study chose a more recognized cut-off value to improve the accuracy of the conclusion. Fourth, imaging features of the hepatobiliary phase (HBP) were not incorporated in this study due to limitation of the contrast agent, and thus could not be compared with some of the previous studies of MVI-negative HCC patients.[16,18] Therefore, future prospective study with multi-center and larger samples are essential to verify our results.

Conclusion

In conclusion, we constructed a nomogram to predict RFS after curative resection in MVI-negative HCC patients by combining MRI features and inflammatory marker. This predictive model can significantly improve the detection rate of high-risk patients, and assist clinicians in treatment decision-making.

Abbreviations

HCC, hepatocellular carcinoma; NLR, neutrophil-to-lymphocyte ratio; MVI, microvascular invasion; RFS, recurrence-free survival; ROC, receiver operating characteristic; C-index, concordance index; DCA, decision curve analysis; PLR, platelet-to-lymphocyte ratio; LI-RADS, Liver Imaging Reporting and Data System; Gd- DTPA, gadolinium- diethylene-triamine pentaacetic acid; APHE, arterial phase hyperenhancement; BMI, body mass index; AFP, alpha-fetoprotein; ALT, alanine transaminase; AST, aspartate aminotransferase; HR, hazard ratio; CI, confidence interval; AUCs, areas under curve.

Ethics Approval and Informed Consent

The studies involving human participants were reviewed and approved by the ethics committee of the Guangxi Medical University Cancer Hospital (KYB2023130). The study was completed in accordance with the Declaration of Helsinki, and all patient data are treated confidentially. The requirement for written informed consent was waived by the Institutional Review Board in view of the retrospective observational nature of the research. Before Gd-DTPA enhanced MRI and curative hepatic resection, subjects received full information about indications, risks, and alternatives and then signed the written informed consent.

Author Contributions

All authors made a significant contribution to the work reported, whether that is in the conception, study design, execution, acquisition of data, analysis and interpretation, or in all these areas; took part in drafting, revising or critically reviewing the article; gave final approval of the version to be published; have agreed on the journal to which the article has been submitted; and agree to be accountable for all aspects of the work.

Funding

This work was funded by Guangxi Science and Technology Program (AB23026018), Guangxi Clinical Research Center for Medical Imaging Construction (Guike AD20238096), Guangxi Medical University Youth Science Foundation project (GXMUYSF202335) and Guangxi Natural Science Foundation (2023GXNSFAA026249).

Disclosure

The authors report no conflicts of interest in this work.

References

1. Bray F, Laversanne M, Sung H, et al. Global cancer statistics 2022: GLOBOCAN estimates of incidence and mortality worldwide for 36 cancers in 185 countries. *CA Cancer J Clin*. 2024;74(3):229–263. doi:10.3322/caac.21834
2. Llovet JM, Kelley RK, Villanueva A, et al. Hepatocellular carcinoma. *Nat Rev Dis Primers*. 2021;7(1):6. doi:10.1038/s41572-020-00240-3
3. Beaufrere A, Caruso S, Calderaro J, et al. Gene expression signature as a surrogate marker of microvascular invasion on routine hepatocellular carcinoma biopsies. *J Hepatol*. 2022;76(2):343–352. doi:10.1016/j.jhep.2021.09.034
4. Lee S, Kang TW, Song KD, et al. Effect of microvascular invasion risk on early recurrence of hepatocellular carcinoma after surgery and radiofrequency ablation. *Ann Surg*. 2021;273(3):564–571. doi:10.1097/SLA.0000000000003268
5. Chan AWH, Zhong J, Berhane S, et al. Development of pre and post-operative models to predict early recurrence of hepatocellular carcinoma after surgical resection. *J Hepatol*. 2018;69(6):1284–1293. doi:10.1016/j.jhep.2018.08.027
6. Li SH, Mei J, Cheng Y, et al. Postoperative adjuvant hepatic arterial infusion chemotherapy with FOLFOX in hepatocellular carcinoma with microvascular invasion: a multicenter, Phase III, randomized study. *J Clin Oncol*. 2023;41(10):1898–1908. doi:10.1200/JCO.22.01142
7. Jiang H, Wei J, Fu F, et al. Predicting microvascular invasion in hepatocellular carcinoma: a dual-institution study on gadoxetate disodium-enhanced MRI. *Liver Int*. 2022;42(5):1158–1172. doi:10.1111/liv.15231
8. Lee S, Kim SH, Lee JE, et al. Preoperative gadoxetic acid-enhanced MRI for predicting microvascular invasion in patients with single hepatocellular carcinoma. *J Hepatol*. 2017;67(3):526–534. doi:10.1016/j.jhep.2017.04.024
9. Cannella R, Matteini F, Dioguardi Burgio M, et al. Association of LI-RADS and histopathologic features with survival in patients with solitary resected hepatocellular carcinoma. *Radiology*. 2024;310(2):e231160. doi:10.1148/radiol.231160
10. Balkwill F, Mantovani A. Inflammation and cancer: back to Virchow? *Lancet*. 2001;357(9255):539–545. doi:10.1016/S0140-6736(00)04046-0
11. Meri S, Magrini E, Mantovani A, Garlanda C. The Yin Yang of complement and cancer. *Cancer Immunol Res*. 2023;11(12):1578–1588. doi:10.1158/2326-6066.CIR-23-0399
12. Wenpei G, Yuan L, Liangbo L, et al. Predictive value of preoperative inflammatory indexes for postoperative early recurrence of hepatitis B-related hepatocellular carcinoma. *Front Oncol*. 2023;13:1142168. doi:10.3389/fonc.2023.1142168
13. Cho EJ, Yu SJ, Lee YB, et al. Prognostic values of inflammation-based scores and fibrosis markers in patients with hepatocellular carcinoma treated with transarterial chemoembolization. *Diagnostics*. 2022;12(5):1170. doi:10.3390/diagnostics12051170
14. Mano Y, Shirabe K, Yamashita Y, et al. Preoperative neutrophil-to-lymphocyte ratio is a predictor of survival after hepatectomy for hepatocellular carcinoma: a retrospective analysis. *Ann Surg*. 2013;258(2):301–305. doi:10.1097/SLA.0b013e318297ad6b
15. Yunyun W, Wei P, Yunying Q, et al. Preoperative MR imaging for predicting early recurrence of solitary hepatocellular carcinoma without microvascular invasion. *Eur J Radiol* 2021;138:109663. doi:10.1016/j.ejrad.2021.109663
16. Qi Q, Mengtian L, Lei X, et al. A model incorporating histopathology and preoperative gadoxetic acid-enhanced MRI to predict early recurrence of hepatocellular carcinoma without microvascular invasion after curative hepatectomy. *Br J Radiol*. 2023;96(1144): 20220739. doi:10.1259/bjr.20220739
17. Leyao W, Bing F, Dengfeng L, et al. Risk stratification of solitary hepatocellular carcinoma ≤ 5 cm without microvascular invasion: prognostic values of MR imaging features based on LI-RADS and clinical parameters. *Eur Radiol*. 2023;33(5): 3592. doi:10.1007/s00330-023-09484-5
18. Leyao W, Meng L, Bing F, et al. Microvascular invasion-negative hepatocellular carcinoma: prognostic value of qualitative and quantitative Gd-EOB-DTPA MRI analysis. *Eur J Radiol*. 2023; 168:111146. doi:10.1016/j.ejrad.2023.111146
19. Balachandran V, Gonen M, Smith J, et al. Nomograms in oncology: more than meets the eye. *Lancet Oncol*. 2015;16(4):e173–80. doi:10.1016/s1470-2045(14)71116-7
20. Chernyak V, Fowler K, Kamaya A, et al. Liver Imaging Reporting and Data System (LI-RADS) version 2018: imaging of hepatocellular carcinoma in at-risk patients. *Radiology*. 2018;289(3):816–830. doi:10.1148/radiol.2018181494
21. Wei H, Fu F, Jiang H, et al. Development and validation of the OSASH score to predict overall survival of hepatocellular carcinoma after surgical resection: a dual-institutional study. *Eur Radiol*. 2023;33(11):7631–7645. doi:10.1007/s00330-023-09725-7
22. A-Hong R, Peng-Fei Z, Da-wei Y, et al. Diagnostic performance of MR for hepatocellular carcinoma based on LI-RADS v2018, compared with v2017. *J Magn Reson Imaging*. 2019;50(3). doi:10.1002/jmri.26640
23. Ng IO, Lai EC, Ng MM, et al. Tumor encapsulation in hepatocellular carcinoma. A pathologic study of 189 cases. *Cancer*. 1992;70(1):45–49. doi:10.1002/1097-0142(19920701)70:1<45::AID-CNCR2820700108>3.0.CO;2-7
24. Wei H, Zheng T, Zhang X, et al. MRI radiomics based on deep learning automated segmentation to predict early recurrence of hepatocellular carcinoma. *Insights Imaging*. 2024;15(1):120. doi:10.1186/s13244-024-01679-8
25. Dong Z, Huang K, Liao B, et al. Prediction of sorafenib treatment-related gene expression for hepatocellular carcinoma: preoperative MRI and histopathological correlation. *Eur Radiol*. 2019;29(5):2272–2282. doi:10.1007/s00330-018-5882-4
26. Xu X, Zhang HL, Liu QP, et al. Radiomic analysis of contrast-enhanced CT predicts microvascular invasion and outcome in hepatocellular carcinoma. *J Hepatol*. 2019;70(6):1133–1144. doi:10.1016/j.jhep.2019.02.023
27. Kim NR, Bae H, Hwang HS, et al. Preoperative prediction of microvascular invasion with gadoxetic acid-enhanced magnetic resonance imaging in patients with single hepatocellular carcinoma: the implication of surgical decision on the extent of liver resection. *Liver Cancer*. 2024;13(2):181–192. doi:10.1159/000531786
28. Lei Z, Li J, Wu D, et al. Nomogram for preoperative estimation of microvascular invasion risk in hepatitis B virus-related hepatocellular carcinoma within the milan criteria. *JAMA Surg*. 2016;151(4):356–363. doi:10.1001/jamasurg.2015.4257
29. Segal E, Friedman N, Kaminski N, et al. From signatures to models: understanding cancer using microarrays. *Nat Genet*. 2005;37(S6):S38–S45. doi:10.1038/ng1561
30. Kuo MD, Yamamoto S. Next generation radiologic-pathologic correlation in oncology: rad-path 2.0. *AJR Am J Roentgenol*. 2011;197(4):990–997. doi:10.2214/AJR.11.7163

31. Yasui K, Shida D, Nakamura Y, et al. Postoperative, but not preoperative, inflammation-based prognostic markers are prognostic factors in stage III colorectal cancer patients. *Br J Cancer*. 2021;124(5):933–941. doi:10.1038/s41416-020-01189-6
32. Yanagisawa T, Mori K, Katayama S, et al. Hematological prognosticators in metastatic renal cell cancer treated with immune checkpoint inhibitors: a meta-analysis. *Immunotherapy*. 2022;14(9):709–725. doi:10.2217/imt-2021-0207
33. Daniel G, Jack L, Rob R, et al. Neutrophils as potential therapeutic targets in hepatocellular carcinoma. *Nat Rev Gastroenterol Hepatol*. 2022;19(4):257. doi:10.1038/s41575-021-00568-5
34. Chew V, Chen J, Lee D, et al. Chemokine-driven lymphocyte infiltration: an early intratumoural event determining long-term survival in resectable hepatocellular carcinoma. *Gut*. 2012;61(3):427–438. doi:10.1136/gutjnl-2011-300509